Supporting Information

Galvanic-driven deposition of large-area Prussian blue film for flexible battery-type electrochromic device

Yanfang Ding[†, ‡, §], *Huanhuan Sun* [‡, §], *Zhihao Li* [‡], *Chunmei Jia* [‡], *Xiaogang Ding* [‡], *Can Li* [‡], *Jian-Gan Wang*[‡, *], *Zhen Li*[†, ‡, *]

[†] Research & Development Institute of Northwestern Polytechnical University in Shenzhen, Shenzhen 519057, China

[‡] State Key Laboratory of Solidification Processing, School of Materials Science and Engineering, Northwestern Polytechnical University, Xi'an 710072, China

E-mail: wangjiangan@nwpu.edu.cn, lizhen@nwpu.edu.cn

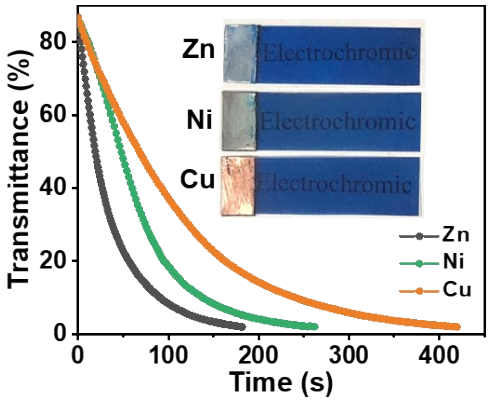

Figure S1 *In-situ* transmittance of depositing the PB films by galvanic-driven with the metal plate of Zn, Ni and Cu at 700 nm.

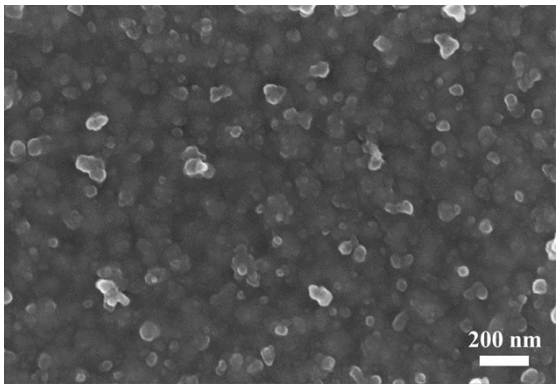

Figure S2 High-resolution SEM image of PB film

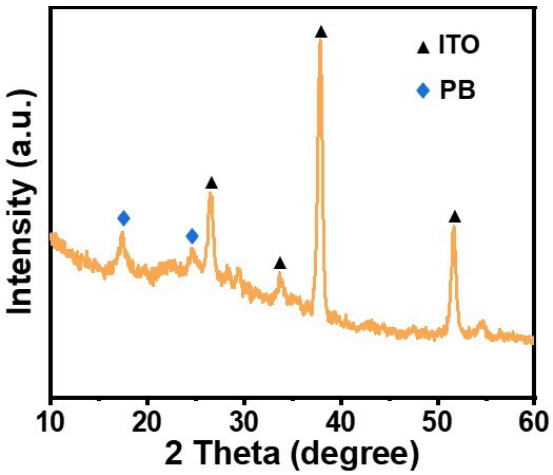

Figure S3 XRD pattern of the PB film on ITO/PET.

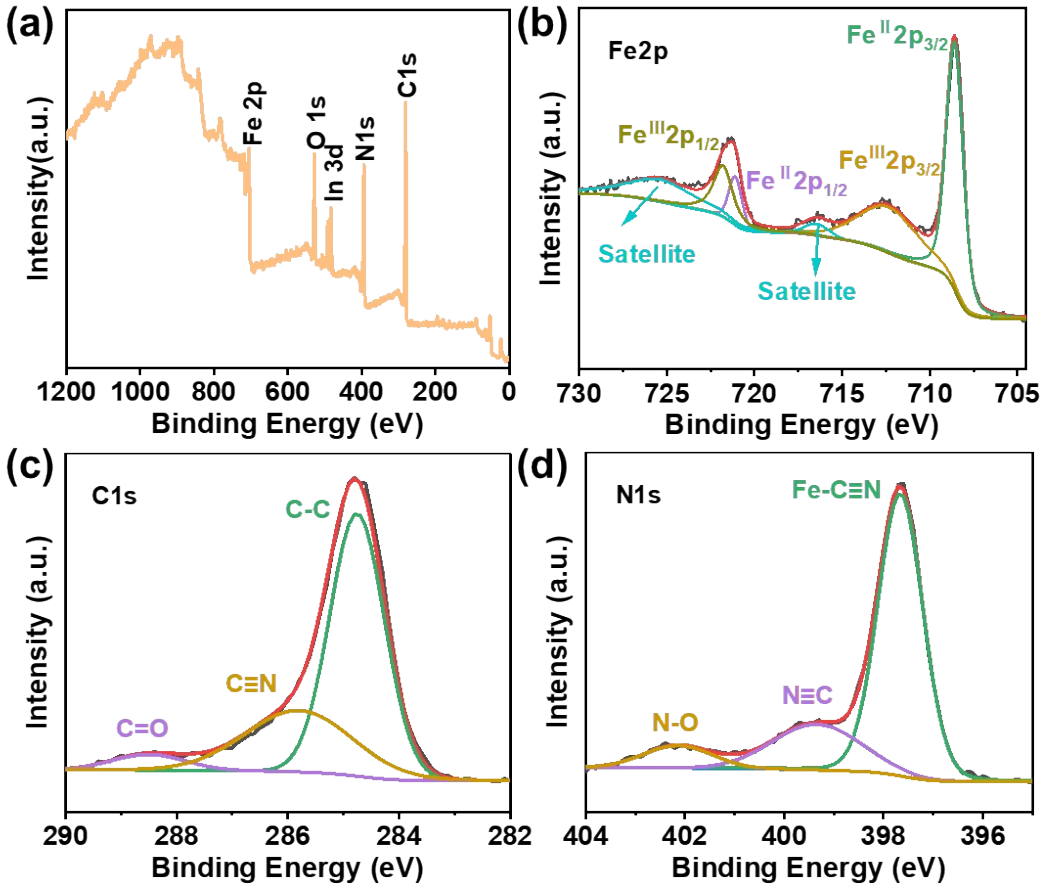

Figure S4 (a) XPS spectra of PB film; High-resolution XPS spectrums of (b) Fe 2p, (c) C 1s, and (d) N 1s.

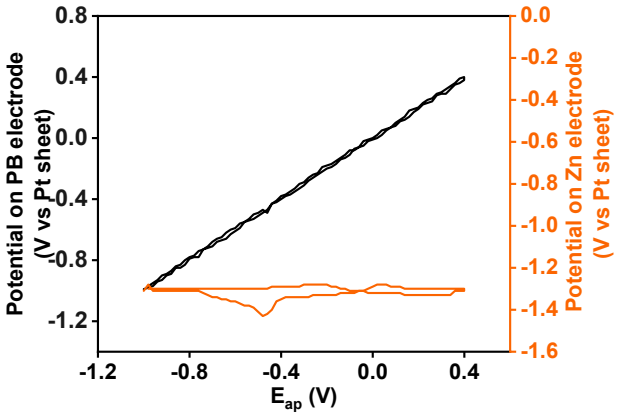

Figure S5. Distribution of the potentials on WE (PB vs Pt reference) and CE (Zn vs Pt reference) according to Eap.

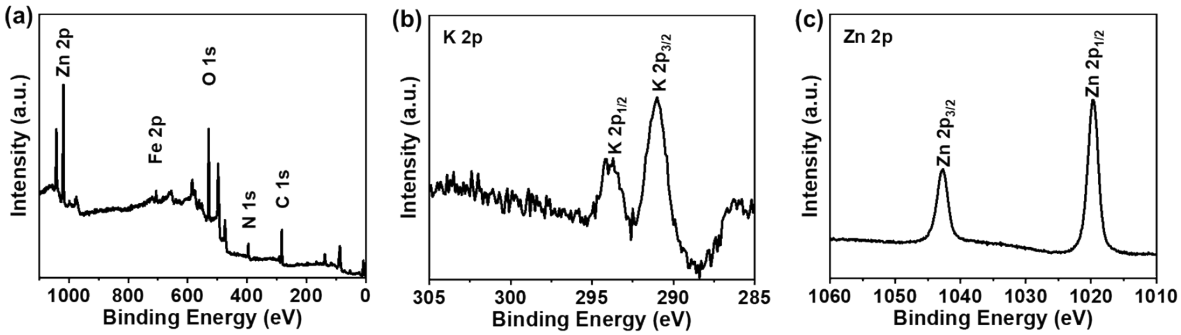

Figure S6 (a) XPS spectra of bleached PB electrode; (b) K 2p and (c) Zn 2p spectra of bleached PB cathode.

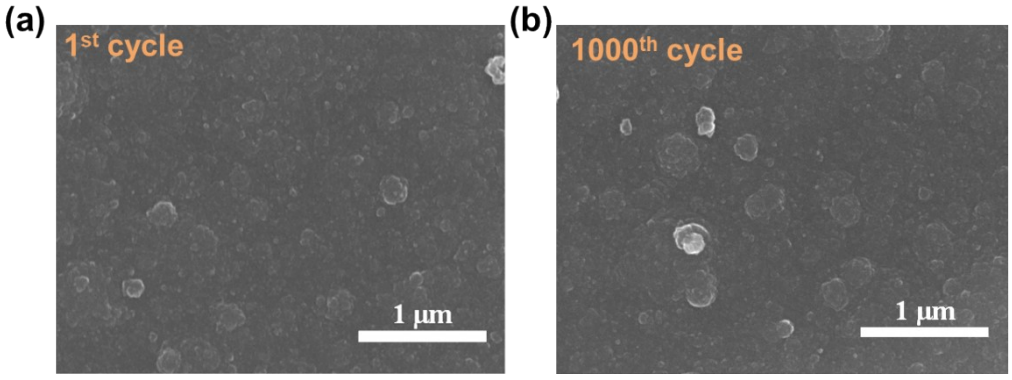

Figure S7 SEM images of PB films after electrochromic cycles: (a) 1st cycle and (b) 1000th cycle.

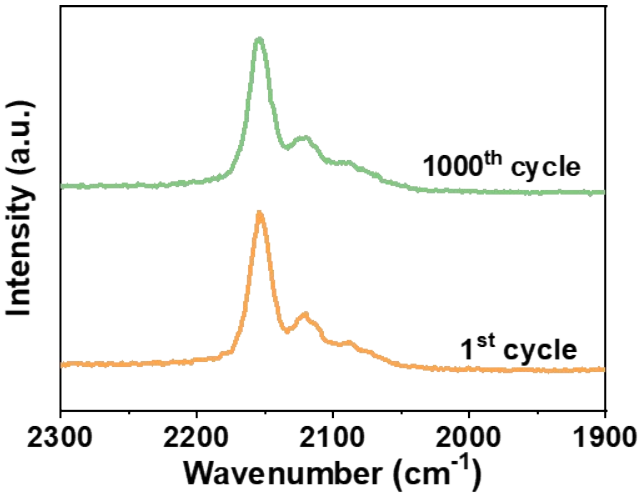

Figure S8 Raman patterns of PB film after 1000 cycles of electrochromic process.

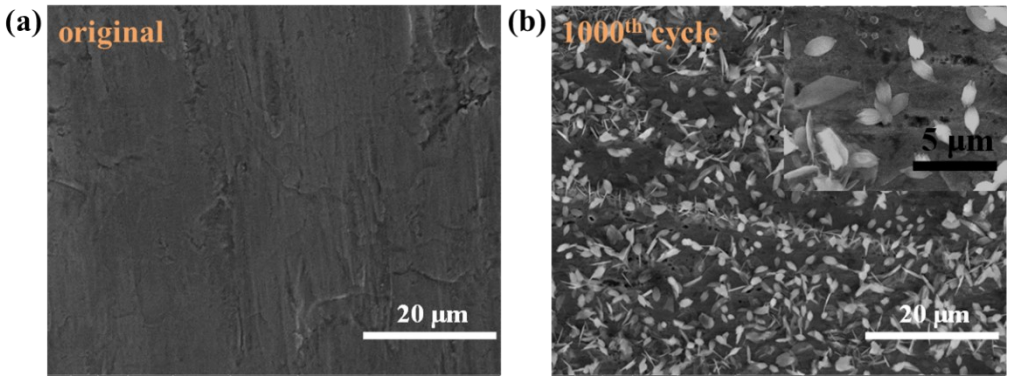

Figure S9 SEM images of Zn electrode of different cycle testing in 1M $ZnSO_4$-KCl solution (a) original state (0 cycle), (b) 1000^{th} cycle.

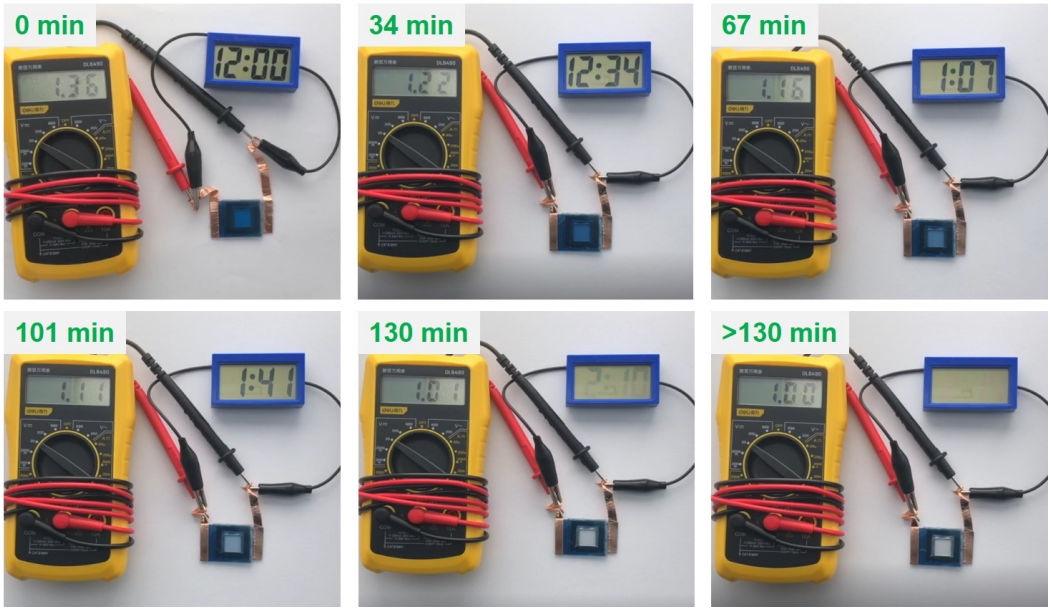

Figure S10 Digital photographs of the PB/Zn device powered electronic clock with liquid crystal display for over 130 minutes.

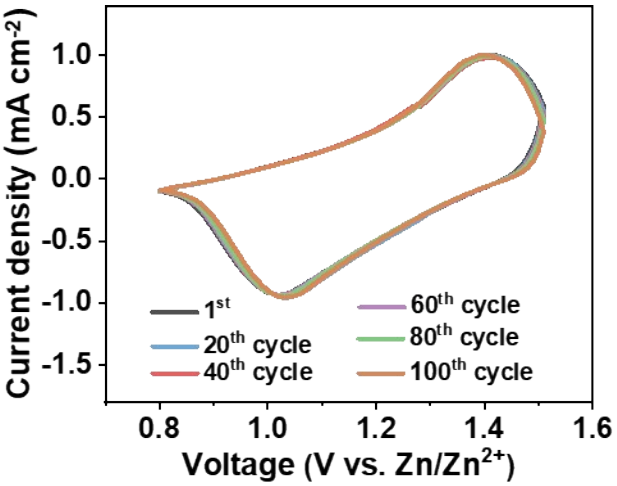

Figure S11 CV curves after 100 cycles mechanical tests under the radius of 15 mm of PB/Zn device.

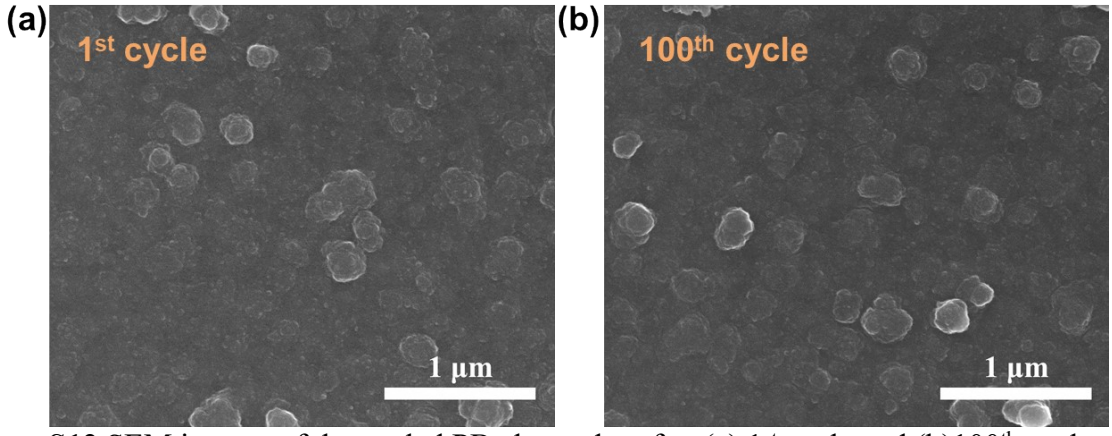

Figure S12 SEM images of the cycled PB electrodes after (a) 1st cycle and (b)100th cycle mechanical tests under the radius of 15 mm.

Table S1. Performance comparison of energy storage type electrochromic devices

Devices	ΔT [%]	Switching time [s] Bleaching/Coloring	Capacity [mAh m^{-2}]	Cycles	Flexibility	Ref.
WO_3-PEDOT/ CeO_2.TiO_2	73.3 (633 nm)	15.8/12.7	25	200	no	[1]
WO_3/Al$(OTF)_3$/InHCF	63 (600 nm)	17.0/47.0	62.8	500	no	[2]
VO_x/Ca$(OTF)_2$/InHCF	41 (600 nm)	--	51.40	260	no	[3]
PB/Al	52.2 (670 nm)	4.1/4.6	~75.0	50	no	[4]
PANI/$ZnSO_4$/Zn PANI/Zn(ClO_4)/Zn	76 (780 nm) 72.2 (780 nm)	3.3/2.7 2.4/2.0	-- 26.4	1000 10000	no	[5]
Mo/Ti:WO_3/Zn	62 (632.8 nm)	-/17.0	150.0	100	no	[6]
V_3O_7/Zn	21 (632.8 nm)	28.6/10.4	310.3	100	no	[7]
WO_3/Zn/ WO_3	75 (633 nm)	7.2/7.4	68	500	no	[8]
WO_3/Zn	88 (632.8 nm)	5.1/3.9	126.3	200	no	[9]
PB/Zn	68.3 (700 nm)	7.5/4.7	77.1	1000	yes	This work

Reference

[1] G. Cai, P. Darmawan, X. Cheng, P. S. Lee, *Adv. Energy Mater.*, 2017, **7**, 1602598.

[2] Z. Tong, R. Lian, R. Yang, T. Kang, J. Feng, D. Shen, Y. Wu, X. Cui, H. Wang, Y. Tang, C.-S. Lee, *Energy Stor. Mater.*, 2022, **44**, 497-507.

[3] Z. Tong, T. Kang, Y. Wan, R. Yang, Y. Wu, D. Shen, S. Liu, Y. Tang, C. S. Lee, *Adv. Funct. Mater.*, 2021, **31**, 2104639.

[4] J. Wang, L. Zhang, L. Yu, Z. Jiao, H. Xie, X. W. Lou, X. W. Sun, *Nat. Commun.*, 2014, **5** , 4921.

[5] Y. Liu, S. Cao, Y. Liang, X. Han, T. Yang, R. Zeng, J. Zhao, B. Zou, *Sol. Energy Mater Sol. Cells*, 2022, **238**, 111616.

[6] H. Li, L. McRae, C. J. Firby, A. Y. Elezzabi, *Adv. Mater.*, 2019, **31**, 1807065.

[7] W. Zhang, H. Li, M. Al-Hussein, A. Y. Elezzabi, *Adv. Optical Mater.*, 2019, **8**, 1901224.

[8] Q. Huang, S. Cao, Y. Liu, Y. Liang, J. Guo, R. Zeng, J. Zhao, B. Zou, *Sol. Energy Mater Sol. Cells*, 2021, **220**, 110853.

[9] H. Li, C. J. Firby, A. Y. Elezzabi, *Joule*, 2019, **3**, 2268-2278.